Design and development of a dual-phase TRIP-TWIP alloy for enhanced mechanical properties

Lola Lilensten* [1, 2], Yolaine Danard[1], Fan Sun[1], Philippe Vermaut[1], Loïc Perrière[3], Jean-Marc Joubert[3], Frédéric Prima[1]

[1] PSL Research University, Chimie ParisTech, Institut de Recherche de Chimie Paris, CNRS UMR 8247, Paris, France

[2]Max-Planck-Institut für Eisenforschung GmbH, 40237 Düsseldorf, Germany

[3]Université Paris-Est, ICMPE (UMR 7182), CNRS, UPEC, 2-8 Rue Henri Dunant, 94320, Thiais, France

Abstract

Triggering transformation induced plasticity (TRIP) and twinning induced plasticity (TWIP) mechanisms in metastable β titanium alloys (bcc, body centered cubic) have helped reaching unprecedented mechanical properties for Ti-alloys, including high ductility and work-hardening. Yet the yield strength of such alloys generally remains rather low. So far, mostly single-phase metastable bcc alloys have been developed. In this study, a dual phase TRIP/TWIP alloy is designed and investigated. While the β-matrix is expected to display TRIP/TWIP deformation mechanisms, the addition of a second phase, α in the present study, aims at increasing the yield strength. The composition was designed in the Ti-Cr-Sn system, based on Calphad prediction and on the semi-empirical *d*-electron alloy design approach. Results were compared to the published full β Ti – 8.5Cr – 1.5Sn (wt%) TRIP/TWIP alloy. The dual-phase alloy was prepared and processed to reach the desired microstructure containing about 20% α. It displays remarkable mechanical properties such as a ductility of 29%, an ultimate tensile strength of 1200 MPa and a yield strength of 760 MPa, 200MPa higher than the reference single-phase β alloy. Analysis of the mechanical properties and deformation microstructures confirm the TRIP and TWIP effects, validating the proposed approach.

Introduction

Knowledge and understanding of the influence on the mechanical properties of the transformation induced plasticity (TRIP), and twinning induced plasticity (TWIP) in β metastable titanium alloys (bcc) are increasing [1], which leads to a rapid development of this new family of Ti-alloys [2–7]. The TRIP effect corresponds to the stress induced formation of martensite, and the TWIP effect relates to the mechanical twinning of the β matrix, mostly in the {332}<113> and the {112}<111> twinning systems. Triggering these mechanisms is correlated to the stability of the β phase: in case of a completely stable β phase, only dislocation glide controls the deformation. Thanks to these additional deformation mechanisms, great mechanical properties including high ductility and work-hardening can be obtained, allowing to overcome a technological threshold for the industrial use of these materials. In spite of such properties, TRIP/TWIP Ti-alloys have a rather low yield strength, usually between 400-600 MPa [4,5,8], which is limiting for possible demanding industrial applications such as the aerospace-related ones. In this context, classical routes to strengthen materials including grain size refinement, solid solution strengthening or precipitation strengthening still remain as possible approaches to increase the yield strength. For dislocation glide controlled plasticity, the Hall-Petch relationship suggests that the smaller the grains, the higher the strength [9]. An increase of the yield strength with decreasing grain size has been confirmed for TWIP and for TRIP Ti-alloys, but it also makes twinning more difficult which leads to a drop in work hardening rate and ductility [10], and may lead to the suppression of the stress-induced martensitic transformation in TRIP alloys [11]. Regarding the solid solution hardening effect, it starts being investigated for some compositions but so far, the increase in the yield strength remains limited [12,13] or is accompanied by a drop in the work hardening rate or the ductility [6,14]. As for the third route, the use of ω nano-precipitates to reinforce the strength of β metastable titanium alloys has raised great interest recently, yet its effect on the ductility and work-hardening is not straightforward [15–17].Considering the possible suppression of TRIP/TWIP in small grain alloys and the limited effect of solid solution strengthening, the aim of this study is thus to go further in the precipitation strengthening strategy to increase the yield strength of a TRIP/TWIP titanium alloy.

As a first proof of concept, the α phase (hcp) is selected as the phase to precipitate in the β-matrix, as it is known to strengthen near β Ti-alloys such as Ti1023 or Ti5553. In order to maintain a deformation mostly controlled by the β phase stability, an amount of about 20% of α phase precipitated in the alloy is targeted. Therefore, the new design challenge relates to a controlled shift of the nominal composition on the Bo-Md stability map, for a given system (Ti-Cr-Sn, in this work). In this way, new compositions may be targeted, keeping the adequate level of β phase metastability to display TRIP and TWIP effects in a precipitation strengthened matrix.

The design approach is first discussed, the alloy is then prepared and processed to reach the desired microstructure, and its mechanical properties and deformation mechanisms are presented in the following.

Materials and experiments

Calphad simulations were performed using the Thermo-Calc software and the published Ti-Cr-Sn database [18]. 200g buttons are prepared by arc-melting. As-cast samples then undergo thermomechanical processes, mainly forging and hot rolling to get square shaped bars. These bars are solution-treated at 1173 K for 900 sec and water quenched to reach a full β microstructure. Specimens are then cold rolled to manufacture sheets, 0.65mm thick, corresponding to a thickness reduction of 80%. Cold-rolled sheets are recrystallized in the β-domain at 1103 K for 1800 sec under high purity Ar atmosphere and then water quenched. From Calphad calculations, equilibrium α phase volume fraction is estimated as a function of the temperature and the targeted α phase fraction is precipitated by a controlled thermal treatment under high purity Ar at 1018K for 1800 sec followed by water quenching. Initial microstructures are characterized by back-scattered electron (BSE) scanning electron microscopy (SEM) and the α phase is quantified by image analyses using the Image J software. The deformed microstructures are analyzed by optical microscopy on Kroll-etched samples using a Keyence instrument, and by electron back scattered diffraction (EBSD) performed on a Zeiss-Crossbeam XB 1540 FIB-SEM instrument (Carl Zeiss) with a field emission gun operated at 15 kV. The EBSD data were collected by an EDAX/TSL data acquisition system. Prior to EBSD observations, the deformed samples are electropolished using a solution of 2-butoxyethanol ($C_6H_{14}O_2$), methanol (CH_3OH), perchloric acid ($HClO_4$) and hydrochloric acid (HCl), held at 278 K. The samples are mechanically characterized by uniaxial tensile tests, carried out at room temperature using an INSTRON5966 machine with a 10kN load cell and an external extensometer with a gauge length of 10mm, at a strain rate of 1.7×10^{-3} s^{-1}, on dog-bone specimens with gauge dimensions of 50 x 5 x 0.65 mm^3.

Results and discussion

Design

The design of the alloy is based on two techniques. First, Calphad predictions are used to predict the amount and composition of the two phases α and β. This is coupled with the semi-empirical *d*-electron alloy design, a design technique that has been developed to predict the β phase stability and thus the TRIP/TWIP behavior of Ti alloys depending on their composition. The *d*-electron alloy design is based on the calculation of the Bo (bond order) and Md (mean energy of the *d* orbitals) parameters for a nominal composition, that have been shown to be a good indicator of the metastability level of the β phase, and therefore its ability to display the desired deformation mechanisms [19]. This last approach has been successfully applied in several studies [3,5,8,12,20]. Recent results reported that in a 100% β state, the Ti - 8.5Cr – 1.5Sn (wt%) alloy with Bo and Md parameters of 2.786 and 2.368 respectively, has a uniform elongation of 0.36 and reaches an ultimate tensile strength of 1260 MPa for a yield strength of 550 MPa, thanks to the TRIP/TWIP mechanisms [3]. Considering these results, the Ti-Cr-Sn system is targeted for the present study, as a “model” system. From the initial composition, Calphad simulations are used to calculate a new nominal composition of a Ti – xCr – ySn alloy for which the β phase, after precipitation of about 20% of α, would have the optimized Ti - 8.5Cr – 1.5Sn composition after chemical partition of alloying element between β and α phases.

Microstructure, mechanical properties and deformation mechanisms

The initial microstructure of the dual-phase alloy is given in Figure 1. The α phase is found as precipitates along the grain boundaries of the β grains and as needles in the matrix. An average surface fraction of 20% of α is confirmed by image analysis,

by averaging the results of multiple images.

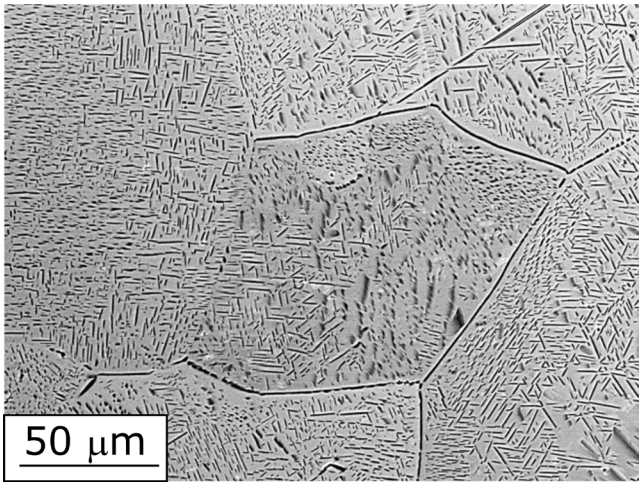

Figure 1: BSE imaging of the initial microstructure prior deformation, evidencing the α precipitation (in dark) in the β matrix (light grey)

The mechanical properties are then characterized, and the tensile curve is given in Figure 2. As a matter of comparison, the tensile curve of the reference Ti – 8.5Cr – 1.5Sn 100% β alloy is given too [3].

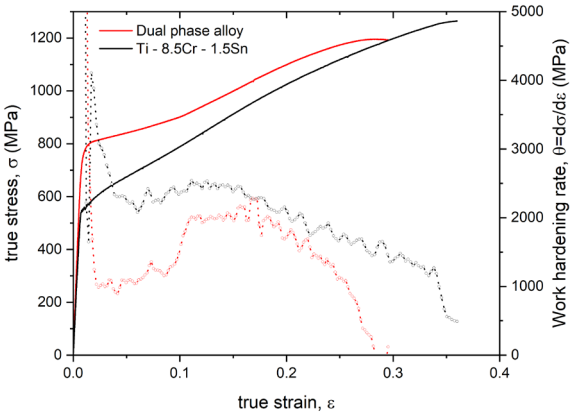

Figure 2: tensile true stress (plain lines) and work-hardening rate (dotted lines) as a function of the true strain for the investigated alloy (in red) compared to the reference Ti – 8.5Cr – 1.5Sn full β alloy (in black) [3]**.**

The dual phase alloy displays, as targeted, a very high yield strength of 760 MPa, combined with an ultimate tensile strength of 1200 MPa and a uniform strain of 0.29. Although the ductility and ultimate tensile strength are slightly reduced (by 60 MPa and 0.07 respectively) compared to the reference 100% β alloy (in black on Figure 2), the main objective to increase the yield strength is fulfilled, with an increase larger than 200 MPa. The obtained tensile curve for the dual phase alloy displays two marked stages, the first one up to strain of about 0.1 and the second one from 0.1 to the rupture. These two stages are reflected by the evolution of the work-hardening rate, that displays a hump with a maximum at a strain of 0.15. Such evolutions are characteristic of TRIP alloys, for which the first stage is mainly related to the formation of stress induced martensite, and the second one is the plastic deformation of the martensite and the residual matrix. Although in TRIP/TWIP alloys, the interplay of the various mechanisms happening simultaneously makes the deformation scheme less straightforward, it has been confirmed that martensite is indeed formed in large quantity during this first stage for such complex alloys [2]. Thus, these mechanical results tend to indicate the formation of martensite under stress. The lower strain hardening rate of the new alloy compared to the reference one in the first stage may suggest a stronger contribution of the martensite, so possibly a higher tendency for TRIP for the new alloy compared to the reference one. However, although slightly lower, the work-hardening of the dual phase alloy remains very high, with a Considere criterion at ε=0.25. The deformation mechanisms of the new alloy are then investigated.

Figure 3 shows the microstructure of the alloy after a deformation of 5%. The sample was polished prior deformation and etched after the deformation, revealing in the α phase. One can see that the deformed β grains contain several deformation bands oriented in different directions within a single grain, looking similar to what is observed in TRIP/TWIP Ti-alloys [11].

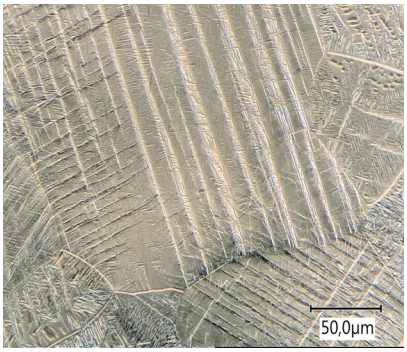

Figure 3: Optical microscopy analysis of the surface of a tensile specimen after 5% deformation

Additional EBSD analyses were performed to better characterize the deformation features and are displayed in Figure 4.

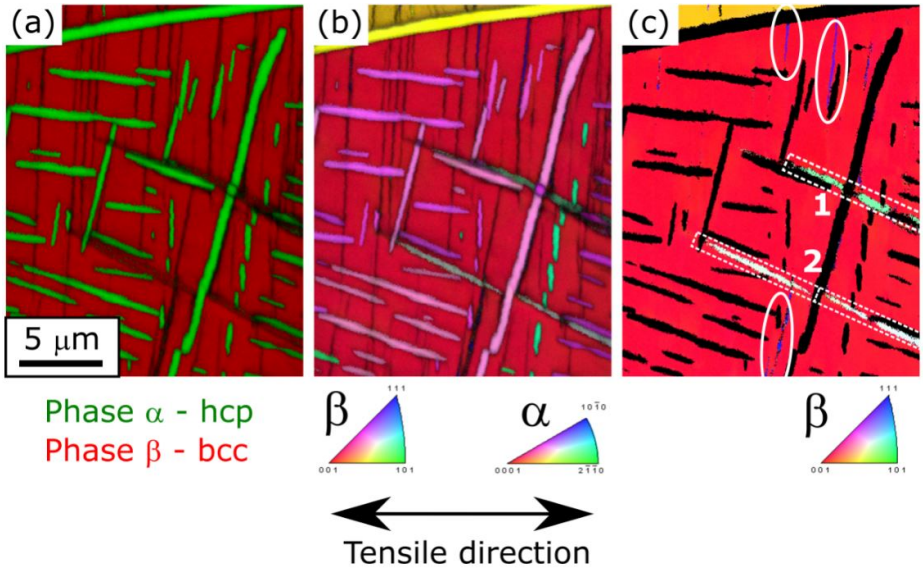

Figure 4: EBSD analysis of a tensile specimen after 5% deformation. (a) phase map superimposed with the image quality map. (b) orientation map for the β and the α phase, superimposed with the image quality map. (c) image quality map for the β phase, highlighting the presence of three {332}<113> twin variants (CSL Σ11) (in white plain ovals – blue- and dashed rectangles – white and green-).

Additional EBSD analyses were performed to better characterize the deformation features and are displayed in Figure 4. Considering the complex structure, the expected presence of 3 crystalline phases (α, β and the martensite α''), and the difficulty to differentiate α and α'', only α and β were indexed in the present case. The phase map (Figure 4a) confirms the presence of α at the grain boundaries and inside the grains, for a total surface fraction of 20%. Figure 4b shows the presence of several thin deformation bands within the β matrix. For a better understanding, the orientation map of the β phase only is given in Figure 4c. Two directions are found for these bands, as indicated by the plain white ovals and the dashed white rectangles. Crystallographical analyses using the CSL relationships allow to characterize a {332}<113> twinning relationship between these features and the matrix. These twins confirm the TWIP effect in this new dual phase alloys. Two different interactions are observed between the twins and the precipitates. The "1" on Figure 4c shows a zone where α is sheared by the twin and changes orientation (see Figure 4b). The "2" on Figure 4c shows a twin that is stopped by the precipitate, and starts again on the other side. Wether these are a single twin or 2 separate twin bands remains unclear. The precipitate remains unchanged. Due to the complex indexation, the martensite cannot be characterized in this analysis, but its formation is strongly suggested by the shape of the tensile curve.

Conclusion

Overall, a new strategy consisting in precipitating a second phase was proposed to increase the yield strength of TRIP/TWIP Ti-alloys. An alloy was designed and processed. Its microstructure consists of large β grains containing a large amount of needle-like α-precipitates, for a total of about 20% (surface fraction) of α. The main objective to increase the yield strength is fulfilled, with an increase higher than 200 MPa for a minor loss of ductility and ultimate tensile strength compared to a reference Ti – 8.5Cr – 1.5Sn 100% β TRIP/TWIP alloy. The study of the deformation mechanisms appears rather complex, due to the interplay of several features that lead to extremely complex microstructures even at low deformation levels. Yet, the first EBSD results confirms the formation of {332}<113> β twins, and the formation of stress induced martensite is suggested by the shape of the tensile curve, and the hump of the work-hardening rate curve, which validates the design of a dual phase TRIP/TWIP alloy.

The hypothesis that precipitating α to increase the yield strength for a β alloy, while maintaining the TRIP and TWIP effects is confirmed and efficient. These first results open the way for future alloy development based on precipitation strengthening. The approach presented here may also be rationalized with systematic coupling of thermodynamic data and Bo-Md predictions.

References

[1] P. Castany, T. Gloriant, F. Sun, F. Prima, Comptes Rendus Phys. 19 (2018) 710–720.

[2] L. Lilensten, Y. Danard, C. Brozek, S. Mantri, P. Castany, T. Gloriant, P. Vermaut, F. Sun, R. Banerjee, F. Prima, Acta Mater. 162 (2019) 268–276.

[3] C. Brozek, F. Sun, P. Vermaut, Y. Millet, A. Lenain, D. Embury, P.J. Jacques, F. Prima, Scr. Mater. 114 (2016) 60–64.

[4] M. Marteleur, F. Sun, T. Gloriant, P. Vermaut, P.J. Jacques, F. Prima, Scr. Mater. 66 (2012) 749–752.

[5] F. Sun, J.Y. Zhang, M. Marteleur, T. Gloriant, P. Vermaut, D. Laillé, P. Castany, C. Curfs, P.J. Jacques, F. Prima, Acta Mater. 61 (2013) 6406–6417.

[6] S. Sadeghpour, S.M. Abbasi, M. Morakabati, A. Kisko, L.P. Karjalainen, D.A. Porter, Scr. Mater. 145 (2018) 104–108.

[7] J. Gao, Y. Huang, D. Guan, A.J. Knowles, L. Ma, D. Dye, W.M. Rainforth, Acta Mater. 152 (2018) 301–314.

[8] F. Sun, J.Y. Zhang, M. Marteleur, C. Brozek, E.F. Rauch, M. Veron, P. Vermaut, P.J. Jacques, F. Prima, Scr. Mater. 94 (2015) 17–20.

[9] N. Hansen, Scr. Mater. 51 (2004) 801–806.

[10] W.L. Wang, X.L. Wang, W. Mei, J. Sun, Mater. Charact. 120 (2016) 263–267.

[11] S. Sadeghpour, S.M. Abbasi, M. Morakabati, L.P. Karjalainen, D.A. Porter, Mater. Sci. Eng. A. 731 (2018) 465–478.

[12] J. Zhang, J. Li, G. Chen, L. Liu, Z. Chen, Q. Meng, B. Shen, F. Sun, F. Prima, Mater. Charact. (2018).

[13] L. Ren, W. Xiao, C. Ma, R. Zheng, L. Zhou, Scr. Mater. 156 (2018) 47–50.

[14] W. Wang, X. Zhang, J. Sun, Mater. Charact. 142 (2018) 398–405.

[15] M.J. Lai, T. Li, D. Raabe, Acta Mater. 151 (2018) 67–77.

[16] F. Sun, J.Y. Zhang, P. Vermaut, D. Choudhuri, T. Alam, S.A. Mantri, P. Svec, T. Gloriant, P.J. Jacques, R. Banerjee, F. Prima, Mater. Res. Lett. 5 (2017) 547–553.

[17] J. Gao, A.J. Knowles, D. Guan, W.M. Rainforth, Scr. Mater. 162 (2019) 77–81.

[18] Y. Gao, C. Guo, C. Li, Z. Du, J. Alloys Compd. 498 (2010) 130–138.

[19] M. Abdel-Hady, K. Hinoshita, M. Morinaga, Scr. Mater. 55 (2006) 477–480.

[20] M. Ahmed, D. Wexler, G. Casillas, D.G. Savvakin, E.V. Pereloma, Acta Mater. 104 (2016) 190–200.